

## Supplementary Information for: A Hybrid Dielectrophoretic Trap-Optical Tweezers Platform for Manipulating Microparticles in Aqueous Suspension

Carlos David González-Gómez<sup>a,b</sup>, Jose García-Guirado<sup>c</sup>, Romain Quidant<sup>c</sup>,  
Félix Carrique<sup>d,e</sup>, Emilio Ruiz-Reina<sup>b,e</sup>, Raúl A. Rica-Alarcón<sup>a,f,\*</sup>

<sup>a</sup>Universidad de Granada, Department of Applied Physics, Nanoparticles Trapping Laboratory, 18071, Granada, Spain

<sup>b</sup>Department of Applied Physics II, Universidad de Málaga, 29071, Málaga, Spain

<sup>c</sup>Nanophotonic Systems Laboratory, ETH Zürich, 8092, Zürich, Switzerland

<sup>d</sup>Department of Applied Physics I, Universidad de Málaga, 29071, Málaga, Spain

<sup>e</sup>Institute Carlos I for Theoretical and Computational Physics (iC1), Department of Applied Physics II, Universidad de Málaga, 29071, Málaga, Spain

<sup>f</sup>Research Unit "Modeling Nature" (MNat), Universidad de Granada, 18071, Granada, Spain

### 1. COMSOL Multiphysics Model

We performed electrostatics simulations using COMSOL Multiphysics finite-element analysis software to estimate the gradient of the squared electric field generated by the two-ring electrodes before fabricating the chips. To this aim, we used the Electrostatics physics interface. Firstly, we defined the 3D geometry of the model as a box of 1000  $\mu\text{m}$  x 1000  $\mu\text{m}$  with 100  $\mu\text{m}$  height. In doing so, we assumed that at a distance of 500  $\mu\text{m}$ , the perturbation of the electric potential due to the ring electrodes was negligible. The geometry of the ring electrodes was modelled assuming a surface without thickness, with a mean inner diameter of 72  $\mu\text{m}$ , a mean outer diameter of 200  $\mu\text{m}$  and a width of 20  $\mu\text{m}$ . The resulting geometry is shown in Supplementary Information.

To account for the dielectric coverslips, we introduced a dielectric shielding boundary condition on the upper and lower boundaries of the geometry. A zero charge boundary condition was applied on the four sidewalls. Lastly, we fixed the potential on the inner electrode to 0 V and on the external one to 10 V. All these boundary settings are depicted in Supplementary Information.

Once the mesh was defined, a stationary solver was introduced to solve the Gauss's law:

$$\begin{aligned}\nabla \cdot \mathbf{D}_E &= \rho_V \\ \mathbf{E} &= -\nabla V\end{aligned}\tag{1}$$

\*Corresponding author: rul@ugr.es

where  $\mathbf{D}_E$  is the electric field displacement,  $\mathbf{E}$  is the electric field,  $V$  is the voltage or potential difference, and  $\rho_V$  is the volumetric charge density, respectively. We consider zero the electric charge density in the electrolyte.

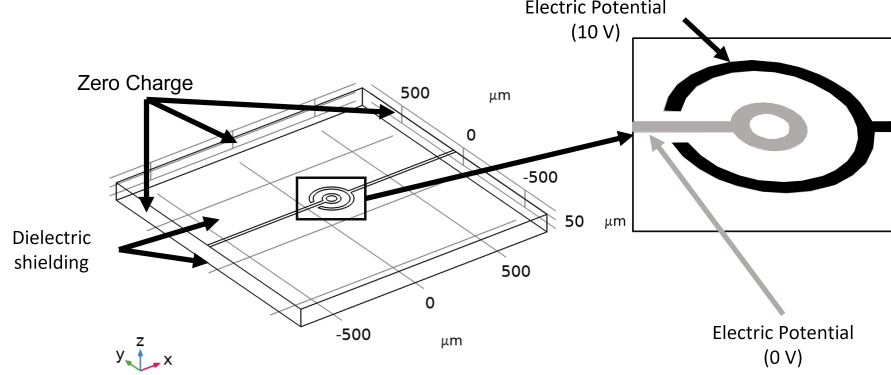


Figure S1: **Model geometry.** Inner and outer diameters are  $72 \mu\text{m}$  and  $200 \mu\text{m}$ , respectively. **Boundary conditions.** A dielectric shielding boundary condition is applied on the upper and lower boundaries. The zero-charge boundary condition is applied on the sidewalls (one remains unmarked for clarity). Regarding the two electrodes, one is set to a 10 V electric potential while the other one is grounded (0 V).

## 2. Description of Supplementary Videos

**Supplementary Video 1** reveals the distribution of particles inside the chamber while the dielectrophoretic trap is activated. In this case, a colloidal suspension composed of  $0.2 \mu\text{m}$ ,  $0.5 \mu\text{m}$ , and  $1 \mu\text{m}$  polystyrene particles is used. We can clearly see an exclusion zone just below the trap, with all the particles populating out of this area. Some  $500 \text{ nm}$  particles are trapped.

**Supplementary Video 2** demonstrates the ability of this platform to selectively trap particles varying the electric field frequency. In this case, we start with three  $3.1 \mu\text{m}$  and four  $0.9 \mu\text{m}$  ProMag particles. The electric field amplitude and frequency were 40 Vpp and 20 MHz, respectively. Once we reduced the frequency to 7 MHz, the smaller particles were expelled. We decreased the electric field frequency to 600 kHz to throw out the others. As explained in the main text, this is due to a different CM factor for each particle size.

**Supplementary Video 3** shows the Dielectrophoretic Trap Modulation. In this experiment, a suspension of  $1 \mu\text{m}$  polystyrene particles is used, and the trapping voltage is modulated as described in the main text. A compressed state is achieved when the potential is high and an expanded state when it is low.

**Supplementary Video 4** shows another example of compression and expansion cycles. In this case, a colloidal suspension composed of  $0.2 \mu\text{m}$ ,  $0.5 \mu\text{m}$  and  $1 \mu\text{m}$  polystyrene particles is used. The applied voltage was  $2 V_{\text{pp}}$  during the expansion step and  $20 V_{\text{pp}}$  during the compression step.

**Supplementary Video 5** depicts the controlled introduction of particles into the dielectrophoretic trap using the optical tweezers platform. A few  $1\ \mu\text{m}$   $\text{SiO}_2$  particles are trapped in different positions in a circular pattern, while many others are confined in the dielectrophoretic trap. Once the laser is switched off, the silica particles are released from the optical traps and are captured by the dielectrophoretic trap.

### 3. Technical Details of the Experimental Setup

Figure S2 provides an picture of the experimental setup. The black background is the holder that supports the microfluidic chamber, which is introduced into the optical tweezers setup. A microfluidic chamber built with a coverslip and the glass slide that incorporates the electrodes (see Methods) was fixed directly onto the holding platform using adhesive tape. The microfluidic chamber can be seen on the centre of the picture. The inset shows an image obtained with a desktop microscope where the electrodes are clearly seen. The electrical connections are ensured welding two gold-coated tungsten wires to microfabricated squared pads with conductive epoxy. The other end of the gold wires are connected by adhesive conductive tape to two alligator clips that clamp the conductive tape. Finally, the alligator clips are connected to the signal generator (not seen in the image).

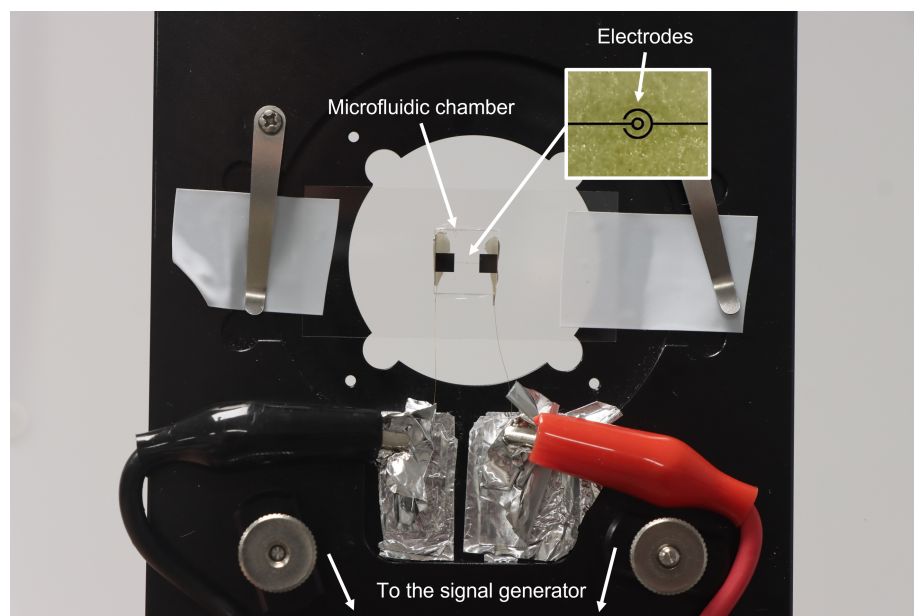


Figure S2: Technical detail of the experimental setup. Note the microfluidic chamber in the centre of the image, and an inset showcasing the electrode architecture. Also, the gold-coated wires can be seen welded to the pads and pasted to the conductive band grasped by the alligator clips connected to the signal generator.